1993

Oscillator Strengths of the Si II 181 Nanometer Resonance Multiplet

Scott D. Bergeson
scott.bergeson@byu.edu

J. E. Lawler

Original Publication Citation

S. D. Bergeson and J. E. Lawler. Oscillator strengths of the Si II 181 nanometer resonance multiplet. Astrophys. J. 414 (2), L137-L140 (1993).

THE ASTROPHYSICAL JOURNAL, 414:L137–L140, 1993 September 10

OSCILLATOR STRENGTHS OF THE Si II 181 NANOMETER RESONANCE MULTIPLET

S. D. BERGESON AND J. E. LAWLER
Department of Physics, University of Wisconsin-Madison, Madison, WI 53706
Received 1993 May 13; accepted 1993 June 24

ABSTRACT

We report Si II experimental log (gf)-values of $-2.38(4)$ for the 180.801 nm line, of $-2.18(4)$ for the 181.693 nm line, and of $-3.29(5)$ for the 181.745 nm line, where the number in parenthesis is the uncertainty in the last digit. The overall uncertainties ($\sim 10\%$) include the 1 σ random uncertainty ($\sim 6\%$) and an estimate of the systematic uncertainty. The oscillator strengths are determined by combining branching fractions and radiative lifetimes. The branching fractions are measured using standard spectroradiometry on an optically thin source; the radiative lifetimes are measured using time-resolved laser-induced fluorescence.

Subject headings: atomic data — ISM: abundances — ISM: atoms — ultraviolet: interstellar

1. INTRODUCTION

Gaseous silicon in the interstellar medium (ISM) is predominantly once ionized and in the ground level. The key atomic transition used to measure Si abundances in the ISM is the 180.801 nm resonance line in Si II. This absorption line is routinely observed in spectra from orbiting observatories such as those from the Goddard High-Resolution Spectrograph (GHRS) aboard the *Hubble Space Telescope* (*HST*).

The relatively convenient wavelength of the Si II resonance line at 180.801 nm is an advantage along with its unusually small oscillator strength. The small oscillator strength causes most of the Si II absorption measurements using this line to be on or near the linear part of the curve of growth. Absorption measurements on the linear part of the curve of growth can be converted to an absolute column density without any knowledge of line shape parameters if an accurate oscillator strength is available. Unfortunately the determination of an accurate (high confidence) oscillator strength for the Si II 180.801 nm line has not been an easy task.

Theoretical work on this oscillator strength has produced values spread over a large range. The upper ^2D level of the transition is a mixture of two configurations, $3s3p^2$ and $3s^23d$, which produces very substantial cancellation in the oscillator strength calculation (Froese Fischer 1976, 1981; Luo, Pradhan, & Shull 1988; Dufton et al. 1983, 1992; Hibbert, Ojha, & Stafford 1992; Nahar & Pradhan 1993). The cancellation which makes the oscillator strength small and thus well suited for probing the ISM also makes it very difficult to calculate with high confidence.

There is also a large spread in previous experimental values for the oscillator strength of the Si II line 180.801 nm based on the electron beam phase shift method (Savage & Lawrence 1966; Curtis & Smith 1974) and absolute emission measurements on an arc (Hofmann 1969). The lifetime of the $^2D_{3/2}$ level is almost too long to be accurately measured using the phase shift method. There are many difficulties in determining an accurate oscillator strength from emission measurements on an arc. The arc must be in local thermodynamic equilibrium, the electron temperature must be accurately measured, a reliable absolute scale must be determined, and the radiometric calibration must be extended into the VUV for the Si II lines. Comparisons of astronomical observations of the weak Si II line at 180.801 nm to stronger Si II lines at shorter wavelengths (Shull, Snow, & York 1981; Van Buren 1986) yield larger values for the oscillator strength than earlier experiments. This kind of comparison is also difficult; the stronger lines are far from the linear region of the curve of growth, and there is a possibility of unresolved component structure and other difficulties (Jenkins 1986).

The best, most broadly applicable method for determining absolute oscillator strengths involves combining emission branching fractions, measured using classical spectroradiometry, with radiative lifetimes, measured using time-resolved laser-induced fluorescence. This modern approach has been used to produce accurate and extensive (almost comprehensive) sets of oscillator strengths for Fe I (O'Brian et al. 1991), V I (Whaling et al. 1985), Sc I, and Sc II (Lawler & Dakin 1989), and many other atoms and ions. We report an emission measurement of the branching fractions for the $3s3p^2\ ^2D_{3/2}$ level. We also report a direct measurement of the radiative lifetime of the $3s3p^2\ ^2D_{3/2}$ and $^2D_{5/2}$ upper levels of the Si II 181 nm resonance multiplet using time-resolved laser-induced fluorescence.

2. BRANCHING FRACTION AND INTENSITY RATIO MEASUREMENTS

The branching fraction experiment is very similar to that used on Cr II and Zn II (Bergeson & Lawler 1993). In the Si II experiment described here, a low-pressure glow discharge used to sputter, ionize, and excite Si is observed through an evacuated path with a 1 m focal length vacuum monochromator. The glow discharge operates at currents from 20 to 95 mA and with a He-Ar gas mixture. A He pressure of 0.2 torr and an Ar pressure ranging from 0.2 to 1.1 torr is used. The Czerny-Turner style monochromator is equipped with a 2400 lines mm^{-1} holographic grating. The reciprocal linear dispersion in the focal plane is nominally 0.41 nm mm^{-1} and the slit widths are adjustable from 5 to 3000 μm. Wavelength scan rates from 0.1 to 100 nm per minute are available. A strip-chart recorder is used to plot the signal from a photomultiplier tube (PMT) located at the exit slit of the monochromator. This simple branching fraction experiment is quite adequate for the relatively few, well isolated lines studied here.

It is not necessary to calibrate the efficiency of the monochromator as a function of wavelength because all of the lines

of interest are all within 1 nm. A PMT with a MgF_2 window and CsTe photocathode is used to ensure the most constant possible efficiency over the 1 nm interval. Spontaneous emission from the glow discharge is unpolarized. The branching fractions are measured for a range of slit widths, discharge currents, and Ar pressures to test for any possible systematic errors. The branching fractions for the 180.801 nm line from the $^2D_{3/2}$ level to the $^2P_{1/2}$ ground level and for the 181.745 nm line from the $^2D_{3/2}$ level to the $^2P_{3/2}$ level are 0.891(5) and 0.109(5), respectively. The number in parenthesis is the uncertainty in the last digit. Hofmann (1969) measured 0.886(8) and 0.114(8), respectively. Hofmann's branching fractions are much more accurate than his absolute oscillator strengths (±25%). It is interesting to note that these branching fractions are significantly different than the Russell-Saunders prediction for a ^2D–^2P multiplet. The Russell-Saunders branching fraction prediction is 0.833 for the $^2D_{3/2}$–$^2P_{1/2}$ transition and is 0.167 for the $^2D_{3/2}$–$^2P_{3/2}$ transition.

The relative populations of the $^2D_{5/2}$ and $^2D_{3/2}$ levels are most probably equilibrated at the gas temperature in the discharge. This is likely because of the long radiative lifetimes of these levels, because of the generally large cross sections for transferring population between nearly degenerate fine-structure levels, and because of the approximately 0.5 torr gas pressure in our experiment. Cross sections for neutral atom collisions to transfer excitation from one fine-structure level to another in the same term of Na were observed to be as large as 1.6×10^{-14} cm^2 by Huennekens & Gallagher (1983). The small 16 cm^{-1} fine-structure splitting of the ^2D term of Si II makes substantial equilibration of the level populations within the term more likely. If the populations of these fine-structure levels are equilibrated, then we can determine the relative radiative lifetimes of the $^2D_{5/2}$ and $^2D_{3/2}$ levels from emission intensity measurements.

The ratio of the emission from the $^2D_{5/2}$ level at 181.693 nm to the total emission from the $^2D_{3/2}$ level at 180.801 and 181.745 nm is measured using our experiment. This ratio is 1.36(3). It is slightly different than what we predict if we assume the $^2D_{5/2}$ and $^2D_{3/2}$ levels have the same radiative lifetimes and if we assume these level populations are equilibrated at the gas temperature in the discharge (~450 K). This ratio therefore suggests that the $^2D_{5/2}$ level has a 4.4% longer lifetime than the $^2D_{3/2}$ level. It is worth noting that Hofmann's (1969) arc emission measurements indicate that the lifetime of the $^2D_{5/2}$ level is 11% longer than that of the $^2D_{3/2}$ level. We will reexamine this question of equilibration of the populations of the fine-structure levels using the lifetime experiment described in the next section.

3. RADIATIVE LIFETIME MEASUREMENT

A few nanosecond duration laser pulse is used to selectively excite the upper level of interest in a time-resolved laser-induced fluorescence (LIF) experiment. The short duration, highly selective laser excitation has a major advantage over both electron beam excitation, and over beam-foil excitation in that the resulting decay curve is a single exponential, free from distortion due to cascade repopulation. If the atom or ion of interest is in a relatively collision-free, optically thin environment, and if it does not escape the observation region before radiating, then the decay time of the single exponential decay curve is the radiative lifetime of the upper level of interest. Such radiative lifetime measurements have already been made for hundreds of levels of many atoms and ions (Lawler 1987). These lifetimes provide the essential normalization needed to convert emission branching fractions into absolute atomic transition probabilities or oscillator strengths.

A rather detailed description of the VUV laser system is available in a recent work on Si I (O'Brian & Lawler 1991). Deep UV and VUV laser radiation is generated by anti-Stokes stimulated Raman scattering of the second harmonic of a pulsed Nd:YAG-pumped dye laser. The most significant change in the VUV laser system is an upgrade of the Nd:YAG pump laser; it now produces 10 ns duration (FWHM), 600 mJ pulses in the second harmonic (532 nm) with a 10 Hz repetition rate.

The fifth-order anti-Stokes radiation is at 180.801 and 181.693 nm when the dye laser fundamental is at 579.15 and 583.74 nm, respectively (vacuum wavelengths). Each nonlinear step in the VUV radiation generation temporally compresses the laser pulse. Fifth-order anti-Stokes radiation has a pulse duration of 4–5 ns (FWHM). The dye laser bandwidth of 0.3 cm^{-1} is slightly increased by the nonlinear steps and by the ac Stark effect in Raman shifting. The bandwidth of the fifth anti-Stokes order is approximately 0.5 cm^{-1}, which is small enough to easily excite single fine-structure levels.

The discharge cell, which is the same used in the branching fraction measurements, operates at pressures of 0.1 to 1.0 torr of Ar during the lifetime experiment. The LIF from the low-pressure discharge cell is detected orthogonally to the laser beam by an f/1 fluorescence collection system and a fast PMT (Hamamatsu R2083Q). The fluorescence collection system is comprised of two MgF_2 lenses which collimate the LIF and then focus the LIF onto the cathode of the PMT. A narrow-band 180 nm interference filter is located between the fluorescence collection lenses where the LIF is roughly collimated. Signals from the PMT are recorded using a Tektronix SCD1000 transient waveform digitizer and are analyzed in a lab computer. Typically the first 50–100 ns after the peak of the fluorescence decay curve is discarded, this eliminates any residual radiation scattered from windows and other surfaces. The remainder of the fluorescence decay curve is fit to a single exponential. Figure 1 is a sample decay curve from this Si II experiment.

Possible systematic errors in time-resolved LIF experiments have been studied and discussed extensively in earlier works

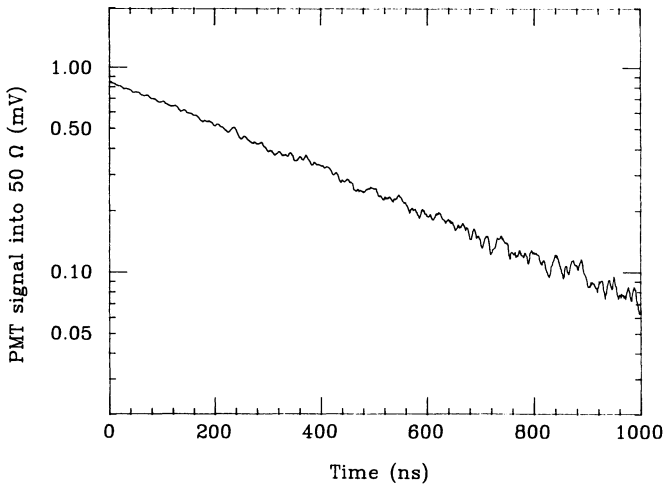

FIG. 1.—Sample decay curve recorded after laser excitation at 181.693 nm of the $3s3p^2\ ^2D_{5/2}$ level.

(e.g., O'Brian & Lawler 1991). The finite electrical bandwidth of the PMT and transient waveform digitizer is a concern for lifetimes in the 2 ns range, but is not a problem for the long (>100 ns) lifetimes studied here. Radiation trapping is completely negligible for a weak transition in an ion. We have searched for effects of radiation trapping in earlier experiments on both ions and neutral atoms with much stronger transitions. Possible distortion of the fluorescence decay curve by Zeeman quantum beats is avoided in this experiment by using a 30 Gauss field to "average out" any quantum beats. The pressure used here (0.1–1.0 torr argon) will also disalign the ions. The possibility of ions escaping from the observation region before radiating is a concern for long-lived (>200 ns) levels. This effect should be greatly suppressed by the 46 mm diameter photocathode which provides a large observation region, and by the argon gas in the cell experiment described here. Atom/ion motion is ballistic in all of our earlier LIF experiments on beams (Lawler 1987; Bergeson & Lawler 1993). Ion motion is diffusive and thus much slower in this cell experiment.

Collisions are the most serious potential source of systematic error. Collisions of the excited Si ions with the argon gas which retard their escape from the observation region might also quench the excited ions. Collisions of the excited Si ions with free electrons in the low-pressure discharge (which is necessary to sputter Si into the gas phase and ionize it) might also quench the excited ions. Extensive measurements of the lifetime of the ^2D levels as a function of pressure and discharge current are made. Sample measurements presented as a Stern-Volmer plot of decay rate (inverse lifetime) as a function of pressure are shown in Figure 2. The data of Figure 2 represent a slice through a three-dimensional plot of decay rate versus pressure and discharge current. Three points need to be made about the data of Figure 2. (1) The observed decay rates after laser excitation of the $^2D_{3/2}$ level at 180.801 nm (*circles*) and after laser excitation of the $^2D_{5/2}$ level at 181.693 nm (crosses) are shown on the same plot. We note that the observed decay rates after laser excitation of these levels are nearly the same. We expect that the populations of the $^2D_{3/2}$ and $^2D_{5/2}$ levels are collisionally coupled in this experiment by neutral atom (Ar) collisions. This means that we cannot claim to have measured the decay rates of the $^2D_{3/2}$ and $^2D_{5/2}$ levels separately; our measurements are probably an average of the reciprocal lifetimes of the $^2D_{3/2}$ and $^2D_{5/2}$ levels with their relative populations determined by their statistical weights and a Boltzmann factor at the gas temperature. (2) Cross sections for neutral atom collision to transfer excitation to levels in other terms should be orders of magnitudes smaller than the 10^{-14} cm^2 typical for population transfer between levels inside a term. The only terms of Si II at nearby or lower energies are the ^4P term and the ground ^2P term. Excitation will not be transferred from the ^2D term to the ^4P term by neutral atom collisions because of the spin selection rule. Only very slight quenching or excitation transfer to the ground term is observed in Figure 2. The straight line in Figure 2 is a linear least-square fit to the data. The slopes determined from this fit, from a similar fit to the 180.801 nm data by itself, and from a fit to the 181.693 nm data by itself are all quite small and all have uncertainties which overlap zero. Although we cannot extract a reliable collisional quenching rate constant from these data, the zero pressure intercept is extremely reliable (~6%). (3) Electron collisional quenching also represents a potential systematic error. The electron density is roughly proportional to discharge current. The decay rate as a function of discharge current from 24 to 116 mA is also measured and extrapolated to zero current. This extrapolation results in a small additional correction to the zero pressure decay rate of Figure 2. A combined analysis of all data from laser excitation of the $^2D_{5/2}$ and $^2D_{3/2}$ levels yields a composite lifetime of 439(44) ns. The overall uncertainty of ±10% includes the random uncertainty (<6%) and an estimate of the systematic uncertainty.

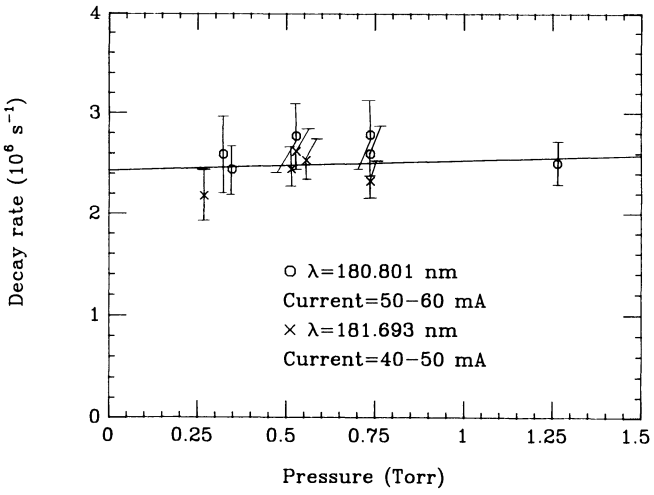

FIG. 2.—Stern-Volmer plot of the ^2D decay rate as a function of Ar pressure in the discharge.

4. RESULTS

The emission experiment described in § 2 indicates that the $^2D_{5/2}$ level has a lifetime 4.4% longer than that of the $^2D_{3/2}$ level. A lifetime of 447 ns for the $^2D_{5/2}$ level and of 428 ns for the $^2D_{3/2}$ level is derived using the relative lifetimes from the emission experiment, the composite lifetime of 439(44) ns from the LIF experiment, and the assumption that the relative population of the $^2D_{5/2}$ and $^2D_{3/2}$ levels are in thermal equilibrium at the gas temperature of the discharge. If our assumption that the populations of the ^2D fine-structure levels are equilibrated is incorrect, then we should be separately analyzing the lifetime data from laser excitation of these two levels. A separate analysis of the data from laser excitation of the $^2D_{5/2}$ level and the $^2D_{3/2}$ level yields lifetimes of 446(45) ns and 410(41) ns, respectively. Our determination of the lifetimes is thus nearly independent of whether or not the fine-structure level populations are equilibrated in the discharge. We find a final lifetime of 447(45) ns for the $^2D_{5/2}$ level and a final lifetime of 420(42) ns for the $^2D_{3/2}$ level.

Our final log (gf)-values and previous theoretical and experimental work on these oscillator strengths are summarized in Table 1. The number in parenthesis is the uncertainty in the last digit. The theoretical results in Table 1 are final values, if provided by the respective authors, otherwise we cited a length approximation result. The length approximation is usually more reliable than the velocity approximation. Good agreement between the length and velocity approximations, which is an indication of accuracy, was achieved in few of the calculations. The calculation of these oscillator strengths is extremely difficult because of the cancellation caused by configuration mixing between the $3s3p^2$ and $3s^23d$ configurations. The reliability of various calculations can also be assessed by

TABLE 1

LOG$_{10}$ (gf)-VALUES FOR THE Si II $3s^2 3p\ ^2P^o$–$3s3p^2\ ^2D$ MULTIPLET

Work	$^2P^o_{1/2}$–$^2D_{3/2}$ 180.801 nm	$^2P^o_{3/2}$–$^2D_{5/2}$ 181.693 nm	$^2P^o_{3/2}$–$^2D_{3/2}$ 181.745 nm	Multiplet
This experiment	−2.38 (4)	−2.18(4)	−3.29(5)	−1.95(4)
Theory				
Nahar & Pradhan (1993)				−2.05
Dufton et al. (1992)	−2.40(12)	−2.19(12)	−3.40(12)	
Hibbert et al. (1992)				−1.97(11)
Luo et al. (1988)	−2.20	−1.96	−2.94	
Dufton et al. (1983)				−2.14
Artru et al. (1981)	−1.59	−1.34	−2.30	
Froese Fischer (1981)				−2.22
Nussbaumer (1977)	−1.71	−1.48	−2.51	
Froese Fischer (1976)				−1.74
Beck & Sinanoglu (1972)				−1.09
Astronomical Observations				
Van Buren (1986)	−1.98(3)			
Shull et al. (1981)	−1.96			
Other Experiments				
Curtis & Smith (1974)[a]	−2.10(5)			
Hofmann (1969)[b]	−2.5(1)	−2.3(1)	−3.3(1)	
Savage & Lawrence (1966)[a]	−2.2(2)			

[a] Phase shift.
[b] Arc emission.

the accuracy in reproducing the experimental splitting of the $3s3p^2\ ^2D$ and $3s^23d\ ^2D$ terms (Dufton et al. 1992). Different theoretical approaches have to some extent converged in recent years toward our experimental values. The modern time-resolved LIF technique we use is more reliable than older experimental techniques.

We are grateful to Prof. Blair Savage of the University of Wisconsin and Donald Morton of the Herzberg Institute for Astrophysics for suggesting this experiment, and urging us to overcome many technical difficulties. This research is supported by the National Aeronautics and Space Administration under grant NAGW-2908.

REFERENCES

Artru, M. C., Jamar, C., Petrini, D., & Praderie, F. 1981, A&AS, 44, 171
Beck, D. R., & Sinanoglu, O. 1972, Phys. Rev. Lett., 28, 945
Bergeson, S. D., & Lawler, J. E. 1993, ApJ, 408, 382
Curtis, L. J., & Smith, W. H. 1974, Phys. Rev. A9, 1537
Dufton, P. L., Hibbert, A., Kingston, A. E., & Tully, J. A. 1983, MNRAS, 202, 145
Dufton, P. L., Keenan, F. P., Hibbert, A., Ojha, P. C., & Stafford, R. P. 1992, ApJ, 387, 414
Froese Fischer, C. 1976, Canadian J. Phys., 54, 740
———. 1981, Phys. Scripta, 23, 38
Hibbert, A., Ojha, P. C., & Stafford, R. P. 1992, J. Phys. B, 25, 4153
Hofmann, W. 1969, Z. Nat., 24, 990
Huennekens, J., & Gallagher, A. 1983, Phys. Rev., A28, 238
Jenkins, E. B. 1986, ApJ, 304, 739
Lawler, J. E. 1987, in Lasers, Spectroscopy, and New Ideas, Vol. 54, Springer Series in Optical Sciences, ed. W. M. Yen & M. D. Levenson (Berlin: Springer), 125
Lawler, J. E., & Dakin, J. T. 1989, J. Opt. Soc. Am., B6, 1457
Luo, D., Pradhan, A. K., & Shull, J. M. 1988, ApJ, 335, 498
Nahar, S. N., & Pradhan, A. K. 1993, J. Phys. B, 26, 1109
Nussbaumer, H. 1977, A&A, 58, 291
O'Brian, T. R., & Lawler, J. E. 1991, Phys. Rev., A44, 7134
O'Brian, T. R., Wickliffe, M. E., Lawler, J. E., Whaling, W., & Brault, J. W. 1991, J. Opt. Soc. Am., B8, 1185
Savage, B. D., & Lawrence, G. M. 1966, ApJ, 146, 940
Shull, J. M., Snow, T. P., & York, D. G. 1981, ApJ, 246, 549
Van Buren, D. 1986, ApJ, 311, 400
Whaling, W., Hannaford, P., Lowe, R. M., Biemont, E., & Grevesse, N. 1985, A&A, 153, 109